*Progress In Electromagnetics Research C, Vol. 63, 209–217, 2016*

# A Slim Composite Antenna with Polarization and Pattern Diversity for WLAN Router Applications

**Li Sun*, Bao-Hua Sun, Guan-Xi Zhang, and Xiao-Le Zhang**

**Abstract**—A slim tri-port antenna with polarization diversity and pattern diversity characteristics is presented for 2.45 GHz WLAN router applications. By composting a J-pole antenna and two perpendicularly crossed dipoles, the proposed antenna achieves available vertical and horizontal polarizations covering the whole horizontal plane. In addition, the two crossed dipoles generate two orthogonal radiation patterns, making it an attractive solution for pattern diversity applications. The three antennas are integrated by overlapping the bottom of J-pole antenna and the top of dipoles, resulting in a slim and compact structure. The proposed antenna is made by copper, with overall volume of only $25.5 \times 25.5 \times 126.5\,\text{mm}^3$. Measured results show that return losses of three ports are all better than 10 dB and isolations between each two ports are better than 20 dB from 2.39 GHz to 2.49 GHz. Furthermore, simple structure, slim size, and light weight make the proposed antenna easy to install vertically on the WLAN routers.

## 1. INTRODUCTION

Indoor wireless radio communication brings a lot of convenience for electronic equipment. Easy setup, mobility, portability, and almost everything about electronic equipment cannot realize without the indoor wireless radio communication. Therefore, a huge development about its systems is done in a few years. Traditionally, indoor wireless radio communication systems need a quarter-wavelength monopole-liked radiation pattern with a null along the vertical axis and an omnidirectional radiation pattern in the horizontal plane. For generating such a radiation pattern, various kinds of antennas [1–3] have been developed for wireless indoor communications. On the other hand, next generation of electronic equipment calls for high speed and high quality data transmission of wireless communication systems. Antenna diversities such as polarization diversity and pattern diversity are effective technique to mitigate signal fading and co-channel interference in multipath environment [4]. With the advantage of saving space and costs, polarization diversity antennas are widely used in many operational systems instead of space diversity antennas. Polarization diversity has the ability to compensate for polarization mismatch due to arbitrary electronic equipment orientation as well [5]. For designing polarization diversity, various kinds of antennas [6–9] have been developed for wireless indoor communications. On the other hand, pattern diversity schemes make use of the incoherence of the rays with sufficiently different angle of arrivals. If the directions of those radiation pattern beams are orthogonal, antennas can collect different rays and hence provide statistically uncorrelated multiple outputs [10]. Therefore, many kinds of pattern diversity antennas [11–13] have been presented for wireless indoor communications.

Motivated by challenging task above, design an antenna with polarization diversity and pattern diversity is an excellent choice for enhancing wireless environment system performance. In this paper, a compact tri-port composite antenna with polarization and pattern diversity is proposed for WLAN

*Received 13 March 2016, Accepted 21 April 2016, Scheduled 5 May 2016*
* Corresponding author: Li Sun (sunli574962432@163.com).
The authors are with the National Laboratory of Science and Technology on Antennas and Microwaves, Xidian University, Xi'an, Shaanxi 710071, China.

router applications. The antenna is a combination of a J-pole antenna and two crossed dipole antennas. When the antenna is placed perpendicular to the ground, the J-pole antenna and two crossed dipoles generate vertical and horizontal polarizations, respectively. Both the vertical and horizontal polarizations are available in the whole horizontal plane. What's more, the radiation beam directions of the two crossed dipole antennas are orthogonal, which indicates that the proposed antenna has the ability to provide pattern diversity characteristics. A prototype of the tri-port antenna is designed, fabricated, and measured. Measured results are in general acceptable with the simulated results. The slim antenna achieves return losses better than 10 dB for all three ports from 2.39 GHz to 2.49 GHz. The isolations between each two ports are greater than 20 dB in the operating band. The overall antenna is made by copper with its size of $25.5 \times 25.5 \times 126.5\,\text{mm}^3$, which is extremely simple and slim, making it easy to be installed vertically on kinds of equipment such as WLAN routers.

## 2. ANTENNA DESIGN

Figure 1(a) shows the geometry of the proposed antenna, which is composed of a J-pole antenna and two crossed dipole antennas. Because of the advantages of being easy to erect, being less costly, and having the lowest angle of radiation, the J-pole antenna is designed to generate the vertical polarization at 2.45 GHz. It consists of a radiator about $0.75\lambda_0$ of length (irregular rectangular strip on the left) and a parallel matching stub about $0.25\lambda_0$ of length (rectangular strip on the right), where $\lambda_0$ is the free-space wavelength at 2.45 GHz. The radiator connects to the parallel matching stub at the end. For generating two orthogonally horizontal polarizations at 2.45 GHz, two perpendicularly crossed dipoles are designed. Each dipole consists of two arms and a rectangular ring, with the feeding port located between the two arms. The arms of the dipole adopt bended structure for size decreasing. The rectangular ring is divided into two parts: one of which is below the feeding point with its length of about $0.5\lambda_0$ and the other of which is above the feeding point. The former part acts as a balun for balancing feed of the bended dipole. The latter part works as the isolation structure between the dipole and J-Pole antenna to increase ports isolation. What's more, it also benefits the impedance matching of the dipole. Since

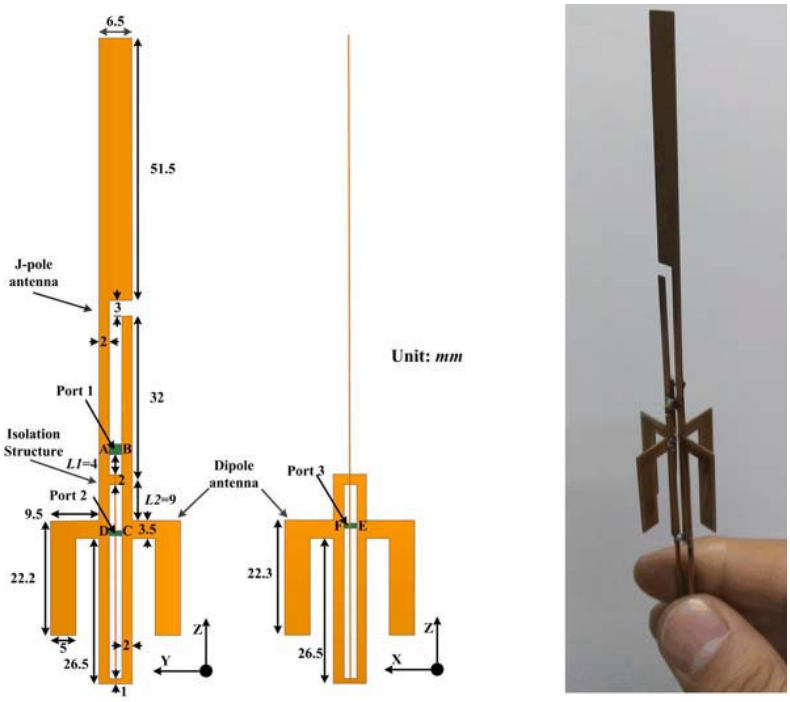


**Figure 1.** (a) Geometry of the proposed antenna. (b) Photograph of the fabricated antenna.

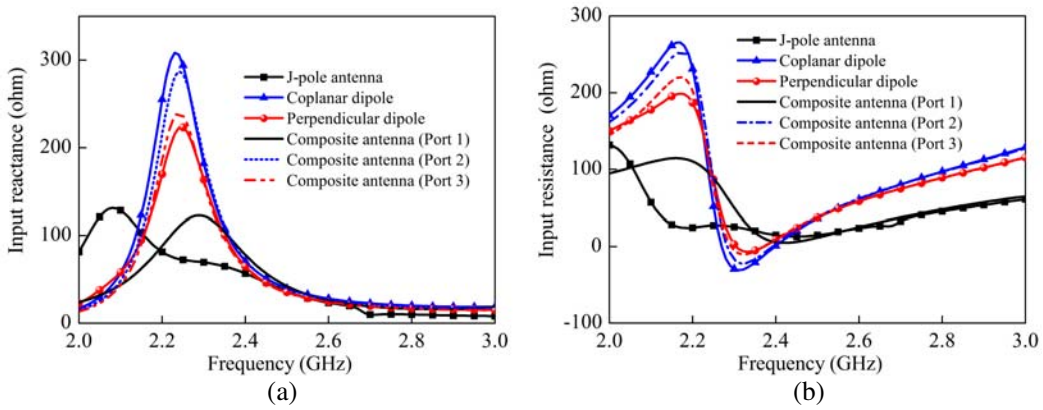


**Figure 2.** Comparison of input impedance between the independent antennas and the proposed composite antenna. (a) Input resistance; (b) input reactance.

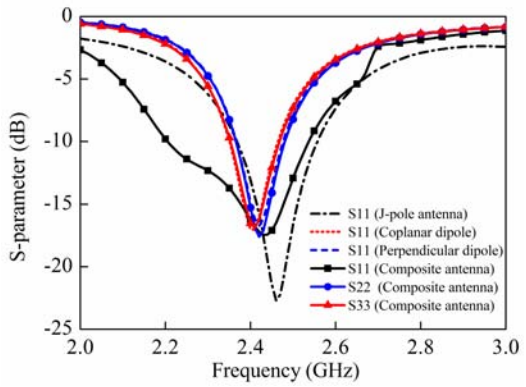


**Figure 3.** Comparison of return losses between the independent antennas and the proposed composite antenna.

the J-Pole antenna requires no DC ground, it can be mounted just about anywhere and still work [14]. Taking advantages of the above characteristics, a composite antenna is designed by combination the J-pole antenna with two perpendicularly crossed dipole antennas. For size reducing and easy fabrication, the end of the J-pole antenna overlaps with the top edge of the coplanar dipole antenna, making the three independent antennas integrate into the proposed composite antenna.

To understand how the integration influences the composite antenna performances, the simulated input impedances of the independent J-pole antenna, two dipole antennas and the proposed antenna are shown in Fig. 2. It can be seen that the input impedances of Port 2 and Port 3 of the composite antenna agree with those of the independent dipole antennas. Port 1 (corresponding with the J-pole antenna) of the composite antenna shows flatter input impedance than the independent J-pole antenna from 2.2 GHz to 2.4 GHz, with smaller variations above 2.4 GHz, indicating that it is easier to achieve good impedance matching in a larger frequency band. Fig. 3 gives the simulated return losses. Comparing with the independent dipole antennas and J-pole antenna, the proposed composite antenna features slight variations for Port 2 and Port 3 and a better 10-dB return loss for Port 1.

## 3. PARAMETER STUDY AND OPERATION PRINCIPLE ANALYSIS

### 3.1. Parametric Study on Impedance Matching

Before carrying out the parametric study, the equivalent circuit of the dipole antenna is studied first. The equivalent circuit of designed bended dipole antenna is shown in Fig. 4. It is based on the classic

five-element equivalent circuit of a dipole antenna [15, 16] in parallel with an inductor and a capacitor between the parallel RLC circuits. In the equivalent circuit, $C_0$ offers the capacitive reactance at lower frequency and $L_0$ works as nullifying the effect of $C_0$ at higher frequency. The parallel circuit section $(C_1, L_1, R_1)$ is a parallel resonant circuit representing the first parallel resonance of the dipole length. They are mainly determined by the length and width of the dipole arm, as well as the bended position. The added series inductor and capacitor $(C_2, L_2)$ are contributed by the portion above the dipole feeding point of rectangular ring. The whole equivalent circuit is easy to change the resonant frequency by tuning the introduced $L_2$ and $C_2$. Thus tuning $L_2$ and $C_2$ improves the impedance matching of the dipole antenna, which is easy to implement by changing the length the rectangular ring above the feeding port of the bended dipole. Element values of equivalent circuits for bended dipole antenna are shown in Table 1. Good agreements between the two input impedance variations are depicted as shown in Fig. 5.

**Table 1.** Element values of equivalent circuit for bended dipole antenna.

| Components | $L_0$ | $C_0$ | $L_1$ | $C_1$ | $R_1$ | $L_2$ | $C_2$ |
|---|---|---|---|---|---|---|---|
| Value | 7.8 nH | 22.9 pF | 10.6 nH | 2.6 pF | 237 Ω | 4.1 nH | 2.9 pF |

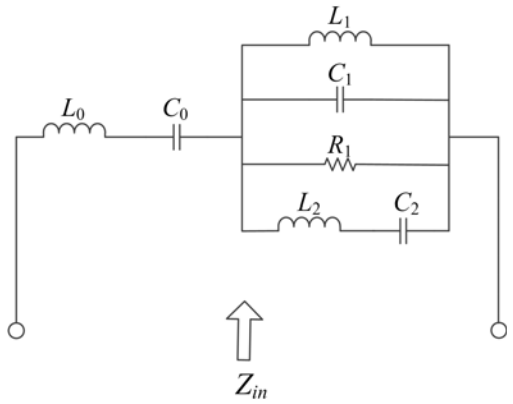


**Figure 4.** Equivalent circuit of the dipole antenna.

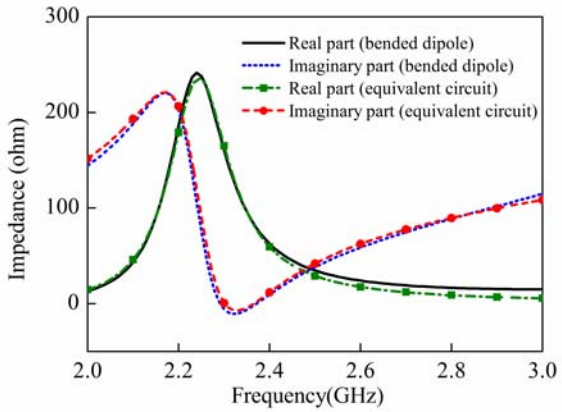


**Figure 5.** Comparison of the input impedances from the equivalent circuit and the simulated bended dipole antenna.

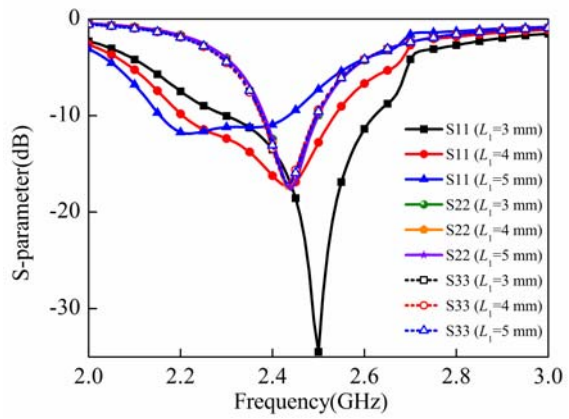


**Figure 6.** Simulated $S$-parameters of the proposed antenna with different $L_1$.

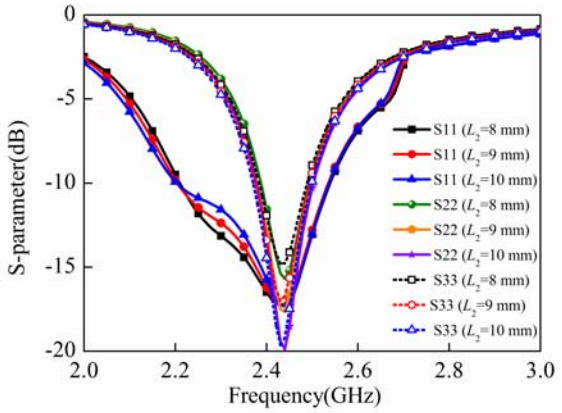


**Figure 7.** Simulated $S$-parameters of the proposed antenna with different $L_2$.

The operating bands of the three ports can be controlled by varying the dimension of the J-pole antenna and the dipole antennas, respectively. To determine appropriate parameters of the proposed antenna, a parametric study is carried out by using Ansoft High Frequency Structure Simulation (HFSS) simulator. Among all these parameters, the distance between the feeding port and the bottom of the J-pole antenna ($L_1$) and the distance between the top and the feeding port of the dipole ($L_2$) are more sensitive to the impedance matching of the J-pole antenna and the dipole antennas, respectively. Thus, $L_1$ and $L_2$ are studied and used to tuning the antenna's return losses. In the parametric studies, only one parameter is adjusted each time, while the other parameters are kept invariant. The simulated S-parameters with different $L_1$ are given in Fig. 6. As can be noticed, with the increasing $L_1$, the resonant frequency of the J-pole antenna shifts to upper band. On the other hand, the return losses of dipole antennas ($|S_{22}|$ and $|S_{33}|$) are insensitive to the variations of $L_1$. Fig. 7 shows the simulated return losses of the proposed antenna with different $L_2$. As the value of $L_2$ increases, the peaks in $|S_{22}|$ and $|S_{33}|$ shift further while little variation on $|S_{11}|$ is made clear. Above all, considering the tradeoff between the antenna height and the $S$-parameters, $L_1 = 4\,\text{mm}$ and $L_2 = 9\,\text{mm}$ are selected.

### 3.2. Surface Current Distribution and Electrical Field Magnitude Distribution

To verify the polarization diversity characteristic, the surface current distributions and the electrical field magnitude distributions of the antenna with different feeding ports are studied. The surface current distributions are shown in Fig. 8. When Port 1 is excited, standing wave currents are mainly distributed

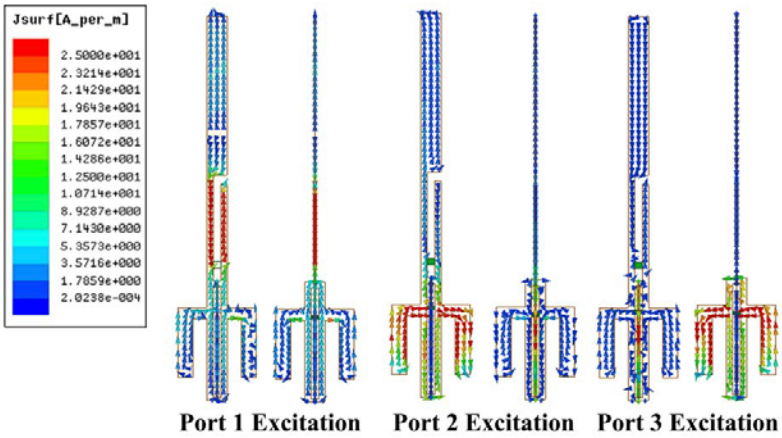


**Figure 8.** Simulated current distributions of the proposed antenna.

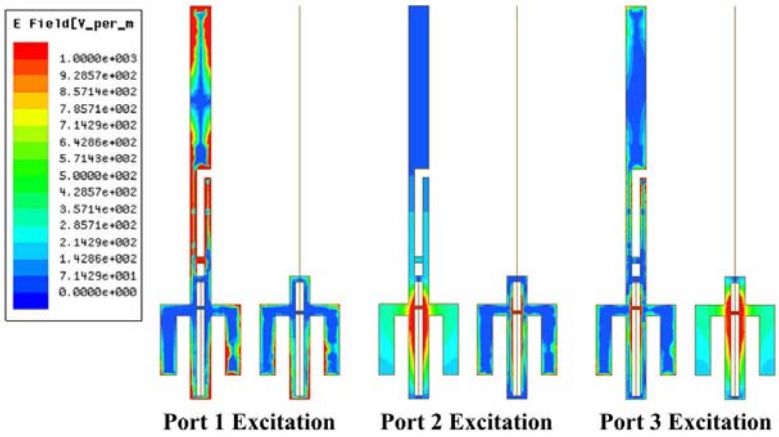


**Figure 9.** Simulated electrical field magnitude distributions of the proposed antenna.

on J-pole antenna while few currents flow through the two dipoles. The isolation structure between Port 1 and Port 2 stops the currents flowing from the J-pole antenna to the dipoles. Since the currents are out of phase at middle of the J-pole radiator, the linear polarization along $z$-axis with the omnidirectional radiation pattern in $XOY$ plane is obtained. When Port 2 is excited, currents mainly flow on the dipole antenna which is coplanar with the J-pole antenna along one direction while few currents flow through the J-pole antenna and the other dipole. Thus, the linear polarization and 8-sharped radiation pattern along $x$-axis are obtained. The similar situation is obtained when Port 3 is excited, generating the linear polarization and 8-sharped radiation pattern along $y$-axis. The electrical field magnitude distributions of the antenna with different feeding ports are given in Fig. 9. As can be seen, it is similar with the current distributions of the proposed antenna. When Port 1 is excited, the maximum electrical field mainly occurs at J-pole antenna. When Port 2 or Port 3 is excited, the maximum electrical field mainly occurs at the corresponding bended dipole antenna.

## 4. SIMULATED AND MEASURED RESULTS

The prototype of the proposed composite antenna has been simulated, fabricated and tested. It is manufactured by copper with thickness of 0.5 mm. The whole area of the antenna is $25.5 \times 25.5 \times 126.5\,\text{mm}^3$. The two crossed dipole antennas are welded together at the top and end of the rectangular ring in the middle. Since the J-pole antenna and the dipole antennas have balanced structures, the composited antenna is directly fed by three coax lines. The outer conductor of the first coax line is connected to the radiator of the J-pole antenna (point A) while the inner conductor of the coaxial cable is connected to the matching stub (point B) for Port 1. The outer conductor and the inner conductor of the second coaxial cable are soldering on two arms of the dipole (point C and D) for Port 2, respectively. Points E and F are connected to the third coaxial cable for Port 3 similarly. The feeding point of Port 3 is moved up 0.5 mm, comparing with Port 2. The fabricated prototype is shown in Fig. 1(b).

Simulated results are obtained by Ansoft HFSS 14.0. For the experimental data, the WILIRON 37269A vector network analyzer and the Near Field Antenna Measurement System Satimo SG 24-S are used. The measured and simulated return losses are shown in Fig. 10. When one port is measured, the other two ports are connected to the 50 Ω matched load. Limited tolerance of the fabrication process and subtle rough surface of the copper may cause slight disagreements between the simulated and measured results. The measured 10-dB impedance bandwidths are 7.3% (2.37 GHz–2.55 GHz), 4.5% (2.38 GHz–2.49 GHz) and 4.5% (2.38 GHz–2.49 GHz) for Port1, Port 2 and Port 3, respectively, all which can cover the desired WLAN band (2.4 GHz–2.484 GHz). The measured and simulated port isolations are shown in Fig. 11. When the isolation between two ports is measured, the third port is connected to the 50 Ω matched load. Results show that the experimental isolations between each two ports are all better than 20 dB across the operating band.

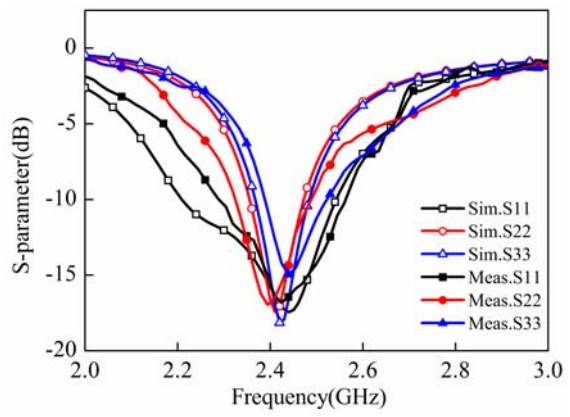


**Figure 10.** Simulated and measured $S$-parameters of the proposed antenna.

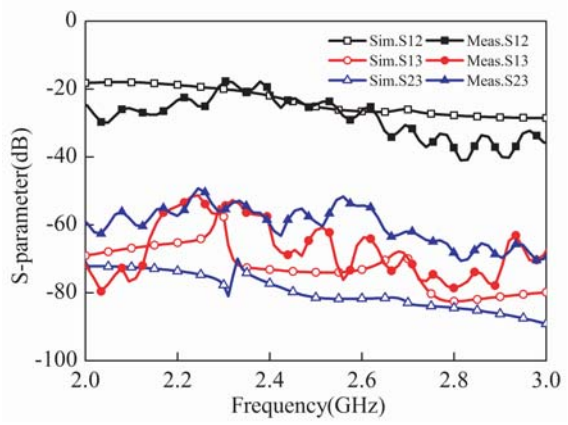


**Figure 11.** Simulated and measured port isolations of the proposed antenna.

The normalized radiation patterns are measured by exciting the proposed composite antenna from each individual port with the other two ports terminated by 50 Ω loads. Figs. 12, 13, and 14 show the measured and simulated far field radiation patterns of the proposed composite antenna for Port 1, Port 2 and Port 3 at 2.45 GHz, respectively. From Fig. 12, it can be seen that when Port 1 is fed, gain variations are less than 0.4 dBi and the cross-polarization remains less than −17 dB in $XOY$ plane. The radiation pattern at $YOZ$ plane is nearly dipole-like, and the cross-polarization within the main lobe keeps less than −17.1 dB. Thus, the vertical polarization with very good omnidirectional performance at $XOY$ plane is obtained.

When Port 2 and Port 3 are excited separately, as shown in Fig. 13 and Fig. 14, the radiation patterns at $XOY$ plane are both 8-shaped, with the main beams orthogonal to each other. Specifically, when Port 2 is fed, the main beams direct at $x$-axis, with the area in the directivity diagram from 45° to 135° and from 225° to 315° satisfying the cross-polarization levels less than −6 dB. When Port 3 is fed, the main beams direct at $y$-axis, with the area in the directivity diagram from −45° to 45° and from 135° to 225° satisfying the cross-polarization levels less than −6 dB. Thus, the effective radiation regions of the two crossed dipoles cover the $XOY$ plane, making the horizontal polarization available in the whole horizontal plane. From the point of radiation pattern, the two crossed dipoles generate two radiation patterns orthogonal with each other, which can provide pattern diversity characteristics.

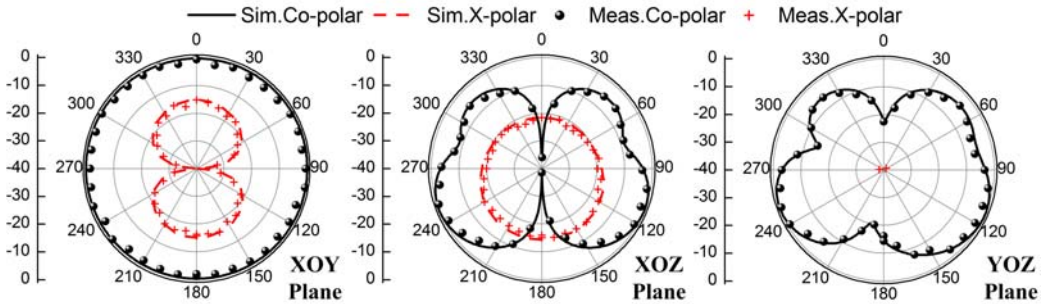


**Figure 12.** Simulated and measured radiation patterns of the proposed antenna (Port 1excitation).

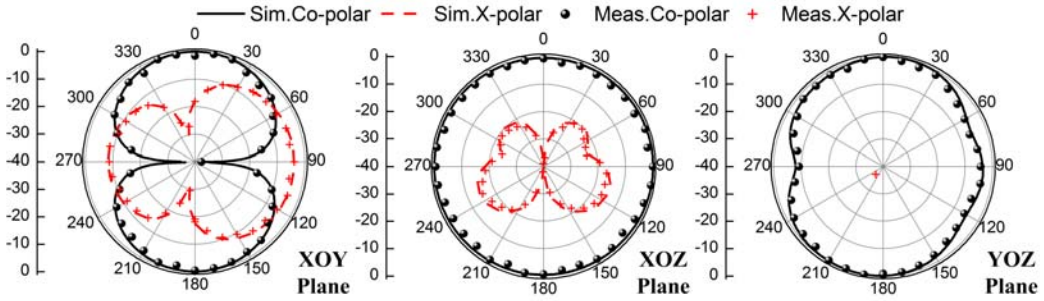


**Figure 13.** Simulated and measured radiation patterns of the proposed antenna (Port 2 excitation).

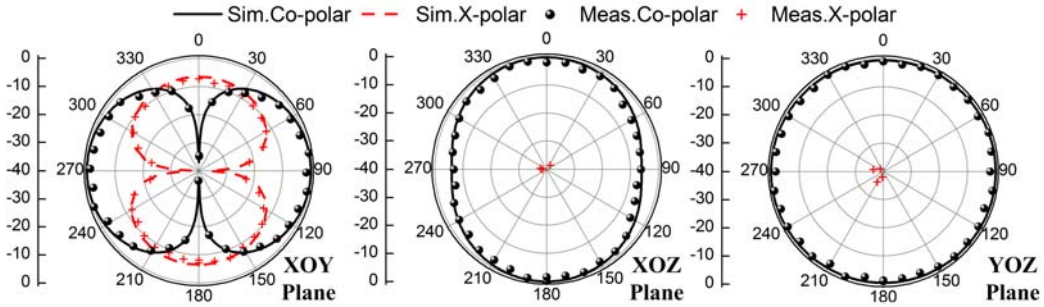


**Figure 14.** Simulated and measured radiation patterns of the proposed antenna (Port 3 excitation).

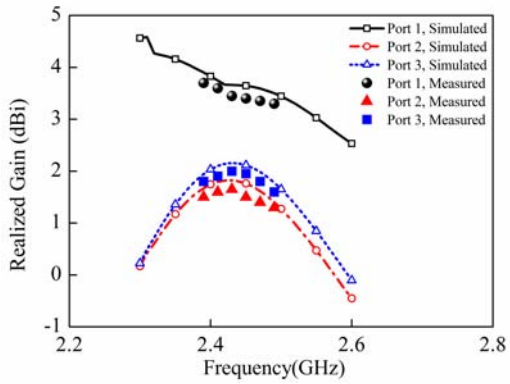


**Figure 15.** Simulated and measured gains of the proposed antenna.

The realized peak gain variations with frequency of the antenna are shown in Fig. 15. The agreements between the measured and simulated results are good. Within the operating frequency ranging from 2.39 to 2.49 GHz, the measured gain varies between 3.3 and 3.7 dBi when Port 1 is excited. Measured gains of Port 2 and Port 3 are 1.3–1.65 dBi and 1.6–2.0 dBi, respectively. The slight decrease in antenna gain is mainly owing to the metallic loss and additional loss of the coaxial lines during the prototype construction and measurement.

In the end, comparisons between the proposed and several reported antennas in terms of impedance bandwidth, size, polarization diversity performance and pattern diversity performance are given in Table 2. It can be seen that the proposed composite antenna presents both polarization and pattern diversity performance. What's more, the extremely slim dimension makes the proposed antenna easy to be installed vertically on kinds of equipment such as WLAN routers.

**Table 2.** Performance comparisons between the proposed and referenced antennas.

| | 10-dB Impedance band (GHz) | Dimension (mm) | Polarization diversity | Pattern diversity |
|---|---|---|---|---|
| Ref [6] | 3.78–4.07 | $100 \times 100 \times 13.9$ | YES | NO |
| Ref [7] | 4.86 | $75 \times 75 \times 1.524$ | YES | NO |
| Ref [8] | 2.38–2.51 | $25.5 \times 126.5$ | YES | NO |
| Ref [11] | 1.88–2.34 | $160 \times 160 \times 17$ | NO | YES |
| Proposed antenna | 2.39–2.49 | $25.5 \times 25.5 \times 126.5$ | YES | YES |

## 5. CONCLUSION

A slim composite antenna with polarization diversity and pattern diversity characteristics for WLAN router applications is proposed in this article. A J-pole antenna and two perpendicularly crossed dipole antennas are combined into a composite antenna to achieve vertical and horizontal polarizations covering the whole horizontal plane. Besides, the two crossed dipoles generate two orthogonal radiation patterns in horizontal plane, which can be worked as pattern diversity. Measured results show that the proposed composite antenna achieves 10-dB return losses from 2.39 GHz to 2.49 GHz for all three ports. The isolation between each two ports is better than 20 dB over the operating band. All these performances of the proposed antenna prove it a good candidate for WLAN router applications, such as reliability improvement in multipath channels and overall average received signal power enhancement.

## REFERENCES


1. Kim, C., J. Jang, H. Lee, Y. H. Jung, et al., "A wideband planar surface wave antenna for the WLAN router," *European Microwave Conf., EuMc 2009*, 1527–1530, Rome, Italy, Oct. 2009.
2. Hsiao, F.-R. and K.-L. Wong, "Omnidirectional planar folded dipole antenna," *IEEE Trans. Antennas Propag.*, Vol. 52, 1898–1902, 2004.
3. Nakano, H., R. Satake, and J. Yamauchi, "Horizontally polarized, omnidirectional antenna with a single feed," *Proc. IEEE Int. Conf. Wireless Information Technology and Systems (ICWITS)*, 1–4, 2010.
4. Zhang, Q.-C., D.-A. Jiang, and W. Wu, "An integrated diversity antenna based on dual-feed cavity-backed slot," *IEEE Antennas Wireless Propag. Lett.*, Vol. 13, 301–304, 2014.
5. Cox, D. C., "Antenna diversity performance in mitigating the effects of portable radio telephone orientation and multipath propagation," *IEEE Trans. Commun.*, Vol. 31, No. 5, 620–628, May 1983.
6. Zou, L., D. Abbott, and C. Fumeaux, "Omnidirectional cylindrical dielectric resonator antenna with dual polarization," *IEEE Antennas Wirel. Propag. Lett.*, Vol. 11, 515–518, 2012.
7. McEwan, N. J., R. A. Abd-Alhameed, E. M. Ibrahim, P. S. Excell, and J. G. Gardiner, "A new design of horizontally polarized and dual-polarized uniplanar conical beam antennas for HIPERLAN," *IEEE Trans. Antennas Propag.*, Vol. 51, No. 2, 229–237, Feb. 2003.
8. Sun, L., G.-X. Zhang, and B.-H. Sun, "Slim planar composite antenna with two orthogonal polarisations for WLAN router application," *Electronics Letters*, Vol. 51, No. 18, 1392–1394, Sept. 2015.
9. Li, Y., Z. J. Zhang, J. F. Zheng, and Z. H. Zheng, "Compact azimuthal omnidirectional dual-polarized antenna using highly isolated collocated slots," *IEEE Trans. Antennas Propag.*, Vol. 60, No. 9, 4037–4045, Sept. 2012.
10. Jungsuek, O. and K. Sarabandi, "Compact, low profile, common aperture polarization, pattern diversity antennas," *IEEE Trans. Antennas Propag.*, Vol. 62, No. 2, 569–576, Feb. 2014.
11. Sun, L., G.-X. Zhang and B.-H. Sun, W.-D. Tang, and J.-P. Yuan, "A single patch antenna with broadside and conical radiation patterns for 3G/4G pattern diversity," *IEEE Antennas Wireless Propag. Lett.*, 1, 2015.
12. Petit, L., L. Dussopt, and J. M. Laheurte, "MEMS-switched parasitic-antenna array for radiation pattern diversity," *IEEE Trans. Antennas Propag.*, Vol. 54, No. 9, 2624–2631, Sep. 2006.
13. Rajo-Iglesias, E., O. Quevedo-Teruel, and M. P. Sánchez-Fernández, "Compact multimode patch antennas for MIMO applications," *IEEE Antennas Propag. Mag.*, Vol. 50, 197–205, Apr. 2008.
14. Choudhury, S. H., M. I. Momtaz, and M. A. Matin, "Analytical deduction of the salient properties of a half wavelength J-pole antenna," *IEEE 2010 International Conference on Computational Intelligence and Communication Networks (CICN)*, 32–35, 2010.
15. Tang, T. G., Q. M. Tieng, and M. W. Gunn, "Equivalent circuit of a dipole antenna using frequency-independent lumped elements," *IEEE Trans. Antennas Propag.*, Vol. 41, No. 1, 100–103, 1993.
16. Hamid, M. and R. Hamid, "Equivalent circuit of dipole antenna of arbitrary length," *IEEE Trans. Antennas Propag.*, Vol. 45, No. 11, 1695–1696, 1997.